IEEE Access
Multidisciplinary | Rapid Review | Open Access Journal

Received March 28, 2022, accepted April 13, 2022, date of publication April 18, 2022, date of current version April 27, 2022.

Digital Object Identifier 10.1109/ACCESS.2022.3168709

Interference Characterization in Cellular-Assisted Vehicular Communications With Jamming

MOHAMMAD ARIF[1], WOOSEONG KIM[1], AND SADIA QURESHI[2]
[1]Department of Computer Engineering, Gachon University, Seongnam 13120, South Korea
[2]School of Data and Electrical Engineering, University of Technology Sydney, Sydney, NSW 2007, Australia

Corresponding author: Wooseong Kim (wooseong@gachon.ac.kr)

This work was supported by the Ministry of Small and Medium-sized Enterprises (SMEs) and Startups (MSS), South Korea, through the Technology Development Program under Grant G21S300458802.

ABSTRACT The automobile industry has been evolving with rapid growth over the last two decades. Conventionally, the narrow band dedicated short-range communications is used for the wireless connectivity of vehicular networks in the automobile industry. However, due to its shorter wireless range, higher latency, and lower capacity; cellular-assisted vehicular communications can be adopted to improve networks performance by disrupting the nearby infrastructure. The performance of cellular-assisted vehicular communications is typically compromised if jammers are present in their vicinity. Thus, it is important to characterize the interference in cellular-assisted vehicular communications with jammers. In this paper, we investigate jamming interference due to clustered-jammers for vehicular networks by considering that vehicles, road-side units, and pedestrians are modeled using an independent one-dimensional Poisson line process while cellular base stations are modeled using an independent two-dimensional homogeneous Poisson point process. The results show that jamming disrupts the performance of the vehicular networks and that this performance is severely compromised by increasing the density of jamming clusters and their transmission power. Therefore, the prime focus of the system designers should be to introduce anti-jamming scenario, when the transmission power and the number of jamming clusters in a network increase.

INDEX TERMS Stochastic geometry, C-V2X communications, Poisson line process, Matern cluster process, vehicular networks, jamming.

I. INTRODUCTION

There has been rapid growth in the automobile industry over the past two decades. The automobile industry facilitates the wireless connectivity of modern vehicular networks to solve issues such as road accidents, traffic congestion, etc. The automobiles can communicate with pedestrians, infrastructures, vehicles, road-side units (RSUs), cloud platforms, etc., and thus, evolve the concept of vehicle-to-everything (V2X) communications [1], [2]. The third-generation partnership project (3GPP) defines cellular V2X (C-V2X) communications as vehicle-to-vehicle (V2V), vehicle-to-infrastructure (V2I), and vehicle-to-pedestrian (V2P) [3], [4] (see, Fig.1). Traditionally, a dedicated PC5 sidelink interface in C-V2X communications can support robust and enhanced network capacity in vehicular communications without requiring the need for cellular infrastructure. This allows vehicular networks to autonomously select their radio resources and communicate in C-V2X communications.

Existing vehicular communications consider the protocols of a narrow band dedicated short-range communications (DSRC) as a standard for V2V communications [5], [6]. However, the DSRC protocol has several limitations in terms of its performance. For instance, in the U.S., the wireless access vehicular environments (WAVE) exploit the DSRC protocol along with the carrier sense multiple access (CSMA); however, the performance of DSRC protocol with CSMA decreases for congested roads due to rapidly changing topology. Moreover, DSRC protocol mainly depends upon the RSUs which are unable to support a variety of vehicular-based applications. Furthermore, due to its short-range, the communication between entities with DSRC protocol is typically restricted to 300 meters [4]. Nevertheless, deploying and managing the infrastructure for RSUs is expensive.

To address the above-mentioned limitations of DSRC protocol in vehicular communications and to provide lower

The associate editor coordinating the review of this manuscript and approving it for publication was Ángel F. García-Fernández.

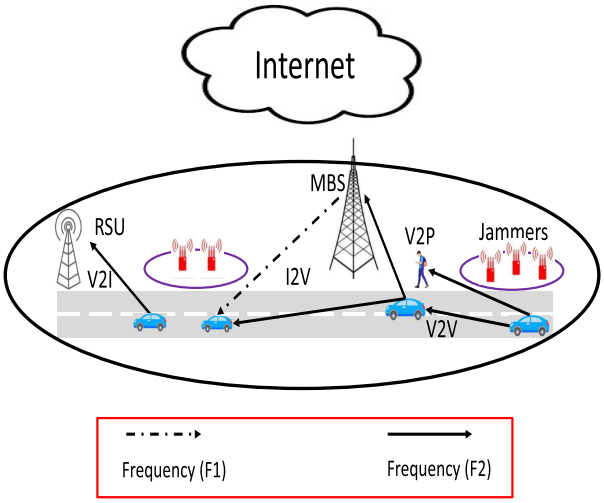

FIGURE 1. Cellular-assisted vehicular communications showing V2V connections, V2I connections, I2V connections, V2P connections, and jammers.

latency with higher reliability and capacity; cellular-assisted vehicular communications have been proposed in several researches [7]–[10], where networks' infrastructure such as cellular BSs is used for vehicular communications. Particularly, C-V2X has been defined in 3GPP and illustrates the key features like direct and cellular-assisted vehicular transmissions. Furthermore, in C-V2X communications, RSUs can be replaced by entities of long-term evolution (LTE) and fifth generation (5G); to reduce management and cost issues.

The performance of the communication technologies in C-V2X communications is often compromised by intentional-jamming attacks [11]–[13]. For instance, communication between a platoon of tanks or armored ground vehicles can be disrupted by jamming attacks, if jammers are intentionally placed in the vicinity. Similarly, the performance of the aerial vehicles can be disrupted by jammers, if jammers are located in the region-of-interest [14], [15]. The most common types of jamming attacks in vehicular communications include denial of service (DoS), Sybil attack, malware, spam, man in the middle attack (MiM), etc. [11], [16]. The jamming attacks in C-V2X communications can pose threats to wireless interface, software, and hardware. Moreover, jammers can also damage the sensors in vehicles and the infrastructure behind the wireless access. Such jamming attacks are very critical and can disrupt the performance of C-V2X communications. Therefore, it is crucial and important to investigate jamming attacks in C-V2X communications for better network performance.

In C-V2X communications, networks' performance is investigated in [17]–[19] without considering the randomness of the vehicular locations and roads which is an important aspect for signal-to-interference ratio (SIR) distribution and coverage-performance. The randomness of vehicles and roads is stochastically modeled in [20], [21] with Matern hardcore point processes (MHPPs). MHPPs consider that vehicles located within a certain radius are not allowed to transmit and that vehicles are distributed in the region-of-interest using a homogeneous 1-dimensional (1D) point process. However, the studies are limited to single lane scenarios and do not consider multi-lane and orthogonal road scenarios. In [22]–[24], authors modeled vehicular networks by considering road segments as a Poisson line process (PLP), vehicles along those roads as an independent 1D homogeneous Poisson point process (PPP), and cellular base-stations (BSs) as an independent 2D homogeneous PPP; and improved the performance of a network. However, the work lacks the performance analysis of C-V2X communications under jamming attacks; which can extensively disrupt networks' performance in terms of its SIR distribution and success in coverage.

In this paper, we consider vehicular communications under intentional-jamming attacks. Previously, intentional-jamming is analyzed for V2V communications in multiple studies [25]–[28]. However, the studies are limited to direct communications. To the best of the authors' knowledge, this is the first research effort to investigate intentional-jamming for cellular-assisted vehicular communications. Particularly, we consider intentional-jamming due to clusters by modeling jammers as a clustering process [14], [15] and investigate networks' performance by modeling cellular BSs as a homogeneous PPP; while vehicles, pedestrians, and RSUs as a PLP [4], [5]. The novel contributions of this paper include i) Investigating the effect of jamming interference due to multiple clustered-jammers in cellular-assisted vehicular communications. ii) Deriving the analytical expression of success probability for V2V, V2I, I2V, and overall success probability of cellular-assisted vehicular communications in the presence of jammers. iii) Evaluating probabilities of association for direct and cellular-assisted vehicular transmission in the presence of jamming interference. iv) Prioritizing focus on anti-jamming when the transmission power of jammers and number of jamming clusters are increased in the network.

The rest of the paper is organized as follows. Section II provides details for the system model of vehicular communications, Section III investigates the success probability of a network with V2V communications, V2I communications, I2V communications, and overall success probability of cellular-assisted V2X transmissions. Section IV presents results and their discussion. Finally, Section V concludes this paper.

II. SYSTEM MODEL

A. INFRASTRUCTURE DEPLOYMENT

Consider a vehicular network comprising of vehicles, RSUs, pedestrians, and cellular macro BSs (MBSs) (see, Fig.2). The road system in vehicular communications is modeled by motion-invariant PLP $\Phi_L = \{L_1, L_2, \ldots, \}$ with line (road) intensity λ_L and is referred in the representation space as $\mathfrak{C} \equiv [0, 2\pi) \times [0, \infty)$ with corresponding line process $\Phi_{\mathfrak{C}}$ and average length per unit space as $\mu_L = \lambda_L/\pi$ [5], [23], [29]. The vehicles are modeled on each line using an independent

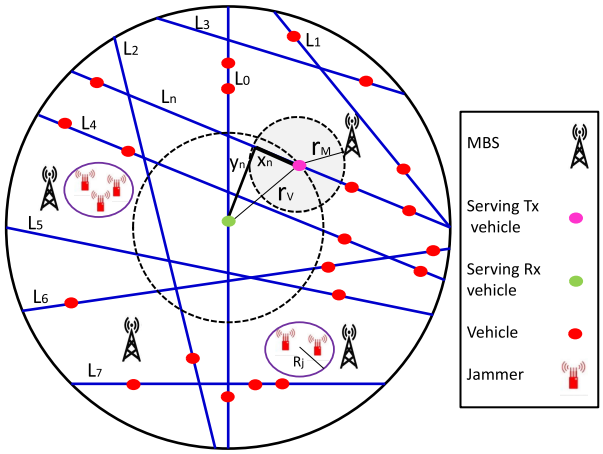

FIGURE 2. Illustration of system model of cellular-assisted vehicular communications.

and 1D homogeneous PPP Φ_v with vehicle intensity μ_v. RSUs and pedestrians are typically located near roads, thus they are also modeled on each line using an independent and 1D homogeneous PPP Φ_u and Φ_p with intensities μ_u and μ_p, respectively. Remind that Φ_v, Φ_u, and Φ_p are stationary point processes and the resulting intensity of these point processes is given by $\mu_V = \mu_v + \mu_u + \mu_p$ [4]. Furthermore, MBSs are modeled using an independent and 2D homogeneous PPP Φ_M with intensity λ_M and it is assumed that at least one vehicle is connected to an MBS in uplink.

Assume that nodes (e.g., vehicles, RSUs, or pedestrians) transmit with probability p independently at a particular frequency such that nodes at each road transmit with intensity $\mu_t = p\mu_V$. Similarly, nodes receive transmissions independently at each road with intensity $\mu_r = (1-p)\mu_V$. Thus, the transmitting and receiving node locations can be modeled with doubly stochastic processes, referred as Φ_t and Φ_r, respectively [4], [23].

By Slivnyak's theorem [29], the distribution of a point process remains the same if a point is translated to origin. Thus, for simple tractability, origin $o \equiv (0,0)$ is translated to the location of a typical receiver. This can be achieved by first placing a point at the origin and passing a line L_o through it using a thinned PLP $\Phi_{L_o} \equiv \Phi_L \cup L_o$ and then, adding a point or a receiving node (e.g., o) at the origin using 1D homogeneous PPP on a line L_o that passes through the origin. The Line L_o is then referred as a typical line. Thus, the thinned point process of transmitting and receiving nodes (i.e., $\Phi_{t_o} \equiv \Phi_t \cup L_o \cup o$ and $\Phi_{r_o} \equiv \Phi_r \cup L_o \cup o$) with density μ_{t_o} and μ_{r_o}, respectively is the superposition of original transmitting and receiving point processes Φ_t and Φ_r with intensities μ_t and μ_r, respectively.

B. JAMMERS DEPLOYMENT

The performance of vehicular communications decreases if jammers are present in the vicinity of jamming site [14], [30]. Typically, low-power ground-jammers are intentionally placed around a jamming site or receiving node in clusters. Thus, the legitimate communication in vehicular networks is disrupted by intentional-jamming created by ground-jammers. Similar to [14], [15], we consider ground-jammers that can jam signals at multiple frequencies (e.g., they can jam F1 and F2 in Fig. 1) and can be modeled using a Matern cluster process (MCP) $\Phi_{\mathcal{J}}$ which consists of parents (or number of jamming clusters) with density λ_j and children (or number of ground-jammers in each cluster) with cluster-radius R_j such that the density of ground-jammers in a network is given as $\lambda_J = \lambda_j \bar{c}$, where $\bar{c}$ is the average number of children (or ground-jammers) per cluster.

C. SIGNAL PROPAGATION

The vehicles, RSUs, and pedestrians transmit with the same power P_V, while the MBSs transmit with the power P_M. The distance-dependent pathloss model is used between transmitting and receiving nodes and the received power decays as $r^{-\alpha_e}$ with propagation distance r, where $\alpha_e > 2$ is the pathloss exponent (i.e., $e \in \{V, M\}$). The channel gain for nodes and MBSs is given as h_V and h_M, respectively that is independent and identically distributed (i.i.d) and is assumed to be slow-flat Rayleigh fading such that the fading gains are exponentially distributed with mean power one [4], [5], [31], [32]. The received signal power from vehicles, RSUs, or pedestrians at a distance r is given as $\mathcal{S}_V = P_V h_V r^{-\alpha_V}$, while the received signal power from MBSs at a distance r is given as $\mathcal{S}_M = P_M h_M r^{-\alpha_M}$. Furthermore, jammers transmit with power P_J. The notations given in this paper are summarized in Table 1.

D. ASSOCIATION POLICY

We consider that a typical receiver associates itself with either an MBS or a vehicular node (such as vehicle, RSU, or pedestrian) based on maximum average received power. This can be obtained by comparing maximum received power from MBSs and vehicular nodes at the typical receiver. For instance, a typical receiver associates with an MBS if $P_M r_M^{-\alpha_M} > P_V r_V^{-\alpha_V}$, otherwise, it associates itself with the vehicular node, where r_M and r_V are the distance between MBS and origin and vehicular node and origin, respectively.

E. SIR OF DIRECT AND CELLULAR-ASSISTED VEHICULAR TRANSMISSIONS

We assume that vehicular networks adopt either direct transmissions (like vehicles transmitting to vehicular nodes) or cellular-assisted vehicular transmissions (i.e., V2I and then I2V) by considering link-distances, environmental impacts, and transmission power. Additionally, we consider the scheme for channel access as a slotted-ALOHA; which approximates the performance of carrier sense multiple access with low- and high-node intensities [21], [33]. Furthermore, similar to [4], we assume that the transmission link in between vehicular nodes and between vehicular nodes and BSs share their resources. Note that we do not exploit PC5-based dedicated sidelink for C-V2X communications

TABLE 1. List of notations.

Notation	Definition
Φ_L	Poisson Line process for Roads
Φ_V	Poisson Point Process for Vehicular Nodes
Φ_v	Poisson Point Process for Vehicles
Φ_u	Poisson point Process for RSUs
Φ_p	Poisson Point Process for Pedestrians
Φ_M	Poisson Point Process for MBSs
$\Phi_{\mathcal{J}}$	Poisson Point Process for Jammers
λ_L	Lines (Roads) Density
μ_V	Vehicular Nodes Density
μ_v	Vehicles Density
μ_u	RSUs Density
μ_p	Pedestrians Density
λ_M	MBSs Density
λ_j	Jamming Clusters Density
P_V	Transmit Power of Vehicular Nodes
P_M	Transmit Power of MBSs
P_J	Transmit Power of Jammers
α_V	Pathloss Exponent of Vehicular Nodes
α_M	Pathloss Exponent of MBSs
h_V	Fading Gain of Vehicular Nodes
h_M	Fading Gain of MBSs
R_j	Jamming Cluster Radius
$\bar{c}$	Average Jammers per Cluster
τ	SIR Threshold
B	System Bandwidth
R	Distance between Origin and network
r_V	Distance between Origin and Vehicular Node
r_M	Distance between Origin and MBS
r_{V2M}	Distance from Vehicular Node to MBS
r_{M2V}	Distance from MBS to Vehicular Node
r	Perpendicular Distance between any Location and any Entity
y_i	Perpendicular Distance from Origin to i-th Line L_i

addressed in 3GPP. Moreover, we consider interference-limited vehicular communications by ignoring thermal noise power and assuming τ as the pre-defined SIR threshold for success in coverage event.

The SIR in the presence of jammers at a typical receiving entity[1] with transmissions $\mathcal{T} \in \{\mathcal{D}, \mathcal{C}\}$, where $\mathcal{D}$ represents direct transmission and $\mathcal{C}$ represents cellular-assisted vehicular transmission and is expressed as

$$\mathrm{SIR}_{\mathcal{T}}(r) = \frac{P_e h_e r^{-\alpha_e}}{\mathcal{I}_e + \mathcal{I}_J}, \tag{1}$$

where P_e is the transmission power of the entities (i.e., vehicles, RSUs, pedestrians, or MBSs), h_e is the fading gain of entities, $\mathcal{I}_e$ is the interference power of entities, and $\mathcal{I}_J$ is the jamming interference at the typical node. Particularly, for direct transmission, the SIR at a vehicular node in the presence of jammers is expressed as

$$\mathrm{SIR}_{\mathcal{D}}(r_V) = \frac{P_V h_V r_V^{-\alpha_V}}{\mathcal{I}_V + \mathcal{I}_J}, \tag{2}$$

where $\mathcal{I}_V$ represents the interference power of vehicular nodes. The SIR for cellular-assisted vehicular transmissions from a vehicular node to an MBS in the presence of jammers is given as

$$\mathrm{SIR}_{\mathcal{C}}(r_{V2M}) = \frac{P_V h_V r_{V2M}^{-\alpha_V}}{\mathcal{I}_V + \mathcal{I}_J}, \tag{3}$$

where r_{V2M} is the distance between a transmitting vehicular node and an MBS. Similarly, the SIR for cellular-assisted vehicular transmissions from an MBS to a vehicular node in the presence of jammers is given as

$$\mathrm{SIR}_{\mathcal{C}}(r_{M2V}) = \frac{P_M h_M r_{M2V}^{-\alpha_M}}{\mathcal{I}_M + \mathcal{I}_J}, \tag{4}$$

where r_{M2V} is the distance between an MBS and a receiving vehicular node and $\mathcal{I}_M$ represents the interference power of the MBSs.

In our system model, we translate origin to the location of a serving (typical) vehicle. Then, we find the serving transmitting (test) vehicle by calculating the maximum received power from all the vehicular nodes at a typical vehicle. Remind that the test vehicle can be located on the same road (i.e., typical line) or on a different road. The test vehicle then finds whether it should transmit to a typical vehicle directly or it should transmit via cellular MBS by calculating maximum received power from a test vehicle at MBS and vehicular node. If the maximum received power at the MBS is smaller then the maximum received power at the vehicular node; the test vehicle considers the direct transmission. While, if the maximum received power at the MBS is larger then the maximum received power at the vehicular node; the test vehicle considers the cellular-assisted vehicular transmission. Generally, there can be interfering transmission entities (like RSUs, vehicles, etc.) inside the disc of $\mathcal{B}(o, r_V)$ and $\mathcal{B}(o, r_M)$ due to transmitter receiver pairs. However, they can be ignored as our focus is the receiver that is present at the origin. After selecting direct transmission, we then calculate SIR and the corresponding success probability using (2) and (27). While, after selecting cellular-assisted vehicular transmission, we then calculate SIR and the corresponding success probabilities using (3) and (29) for transmitting to an MBS and (4) and (31) for transmitting from an MBS.

III. PRELIMINARIES

In this section, we derive distance between vehicular transmitting and receiving nodes and vehicular transmitting and cellular nodes. We also derive association probabilities of the transmitter (test) vehicle with the typical receiving vehicle and cellular BS. Furthermore, we also derive interference of vehicular nodes, cellular nodes, and jammers.

[1]In the rest of the article, entity refers to MBSs, RSUs, pedestrians, and vehicles. While, vehicular nodes refer to RSU, pedestrians, and vehicles.

A. DISTANCE DISTRIBUTION

Here, we derive distance distribution to vehicular nodes and MBSs which will be used in deriving the association probabilities of vehicular transmitting node with vehicular receiving node and MBS.

1) DISTANCE DISTRIBUTION OF VEHICULAR NODES

The probability density function (PDF) of the distance distribution between receiving and transmitting vehicular node is derived in Appendix VI and is expressed as

$$\begin{aligned} f_{R_V}(r_V) &= \frac{d}{dr_V} F_{R_V}(r_V) \\ &= 2\exp\Bigg(-2\mu_V r_V + 2\lambda_L \pi \\ &\quad \times \int_0^{r_V} 1 - e^{-2\mu_V \sqrt{r_V^2 - y^2}} dy \Bigg) \\ &\quad \times \left(\mu_V + 2\lambda_L \pi \int_0^{r_V} \frac{\mu_V r_V e^{-2\mu_V \sqrt{r_V^2 - y^2}}}{\sqrt{r_V^2 - y^2}} dy \right). \end{aligned} \tag{5}$$

2) DISTANCE BETWEEN MBS AND VEHICULAR NODE

The distance between transmitting vehicular node and receiving MBS in terms of its CDF is given as

$$F_{R_M}(r_M) = 1 - \exp(-\pi \lambda_M r_M^2). \tag{6}$$

The PDF of the distance between transmitting vehicular node and MBS is expressed as

$$f_{R_M}(r_M) = 2\pi \lambda_M r_M \exp(-\pi \lambda_M r_M^2). \tag{7}$$

Note that the distance distribution between the vehicular transmitting node and receiving MBS is the same as vehicular receiving node and transmitting MBS.

B. ASSOCIATION PROBABILITIES

Here, we derive the probability of association of the serving (transmitter) test vehicular node with the typical receiving vehicular node or the cellular BS.

1) DIRECT TRANSMISSION PROBABILITY

Direct transmission considers the direct communication of vehicular nodes. The probability that a typical vehicular node located on a typical line will associate with the transmitting vehicular node is referred as direct transmission probability or association probability of a typical receiving vehicular node with the transmitting vehicular node. The direct transmission is selected by the transmitter (test) vehicular node if the average received signal strength at the typical receiving vehicular node is equal or larger than the average received signal strength at the cellular BS. The probability that a typical transmitting vehicular node selects direct transmission by considering distance to vehicular receiving node as r_V is given as

$$\begin{aligned} \mathcal{A}_D(r_V) &= \Pr\{r_V^{-\alpha_V} \geqslant r_M^{-\alpha_M}\} \\ &= \Pr\{r_M \geqslant r_V^{\alpha_V/\alpha_M}\}. \end{aligned} \tag{8}$$

Eq. (8) represents that there is not even a single cellular BS within the radius of $r_V^{\alpha_V/\alpha_M}$ and that vehicular transmitter associates to vehicular receiver located at origin. Thus, the CCDF of (8) is expressed as

$$\mathcal{A}_D(r_V) = \exp\left(-\pi \lambda_M r_V^{-(\alpha_V/\alpha_M)^2}\right). \tag{9}$$

By removing condition on distance r_V and considering network's radius R, we get association probability of a typical receiving vehicular node with the transmitting vehicular node in direct transmission as

$$\mathcal{A}_D = \int_0^R \exp\left(-\pi \lambda_M r_V^{-(\alpha_V/\alpha_M)^2}\right) f_{R_V}(r_V) dr_V. \tag{10}$$

2) CELLULAR-ASSISTED VEHICULAR TRANSMISSION PROBABILITY

Cellular-assisted vehicular transmission considers communication of vehicular nodes by considering cellular BSs of the given infrastructure. The probability that a vehicular transmitting node selects cellular BS for communicating to other vehicular nodes is referred as cellular-assisted vehicular transmission probability. The cellular-assisted vehicular transmission is selected by the transmitting vehicular node if the average received signal strength at the MBS from transmitting vehicular node is larger than the average received signal strength at the typical receiving vehicular node from the transmitting vehicular node. The probability that the transmitting vehicular node selects cellular-assisted vehicular transmission by considering distance to cellular BS as r_M is derived as

$$\begin{aligned} \mathcal{A}_C(r_M) &= \Pr\{r_M^{-\alpha_M} > r_V^{-\alpha_V}\} \\ &= \Pr\{r_V > r_M^{\alpha_M/\alpha_V}\}. \end{aligned} \tag{11}$$

Eq. (11) represents that no vehicular node within a radius of $r_M^{\alpha_M/\alpha_V}$ exists and that vehicular transmitter associates to cellular BS. The association probability of the cellular-assisted vehicular transmission can be obtained from CCDF of r_V using (38) (i.e., $1 - F_{R_V}(r_V)$) and by removing condition on distance r_M. It is then expressed as

$$\begin{aligned} \mathcal{A}_C = &\int_0^R \exp\left(-2\pi \lambda_L \int_0^{r_M^{\alpha_M/\alpha_V}} 1 - e^{-2\mu_V \sqrt{r_M^{\alpha_M/\alpha_V\,2} - y^2}} dy \right) \\ &\times \exp\left(-2\mu_V r_M^{\alpha_M/\alpha_V}\right) f_{R_M}(r_M) dr_M. \end{aligned} \tag{12}$$

C. INTERFERENCE CHARACTERIZATION

Here, interference of vehicular nodes located on a typical line (road), interference of vehicular nodes located on roads excluding a typical line, and interference of cellular BSs is derived in terms of Laplace transform of interference. Moreover, interference of jammers in terms of jamming interference is also derived.

Conventionally, for vehicular networks, interference at a typical node originates from entities such as vehicular nodes

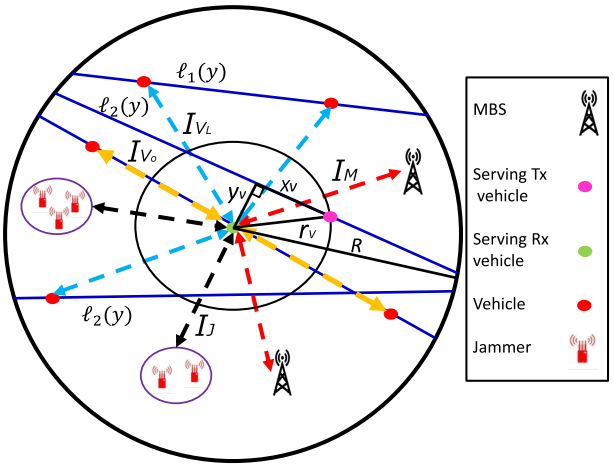

FIGURE 3. Interference at a typical vehicle where dashed lines represent interference of vehicular nodes, cellular BSs, and jammers.

located on all other lines (roads) excluding a typical line (referred as I_{V_L}), vehicular nodes located on a typical line (referred as I_{V_o}), and cellular BSs (referred as I_M) (see, Fig. 3). We characterize each of them separately.

1) INTERFERENCE OF VEHICULAR NODES LOCATED ON ROADS (EXCLUDING A TYPICAL ROAD)

Here, we derive interference of vehicular nodes located on all other roads excluding a typical line (road). This can be obtained by first deriving interference from a single road (excluding a typical road) and then obtain the results for all the other roads (excluding a typical road).

The interference originating from a single road excluding a typical road is referred as I_{V_L} and is derived by considering that the perpendicular distance y from origin to that road is either greater than r_V or less than r_V. If $y \geqslant r_V$, all the vehicular nodes located on the considered line $[-\sqrt{R^2-y^2}, \sqrt{R^2-y^2}]$ (referred as ℓ^*) will take part in the interference process (i.e., $\ell_1(y)$). Whereas, if $y < r_V$, then only those vehicular nodes on the considered line that are located outside $\mathcal{B}(o, r_V)$ but inside $\mathcal{B}(o, R)$ (i.e., $[-\sqrt{R^2-y^2}, -\sqrt{r_V^2-y^2}]$ and $[\sqrt{r_V^2-y^2}, \sqrt{R^2-y^2}]$ referred as ℓ^{**}) will take part in the interference process (i.e., $\ell_2(y)$). we first derive interference from a single road in terms of $\ell_1(y)$ and then $\ell_2(y)$. Later on, we obtain the interference originating from all such roads excluding a typical road.

The interference of a single road lying in a disc $\mathcal{B}(o, R)$ has a road length of $2\sqrt{R^2-y^2}$ between vehicles and horizontal distance of x. Conventionally, interference from vehicular nodes at a typical receiver is expressed in terms of a Laplace transform of interference $L_I(s) = \mathbb{E}[e^{-Is}]$, where $s = P_e y^{\alpha_e}$. Thus, interference originating from k vehicles at a typical receiver residing on the road length $2\sqrt{R^2-y^2}$ under Rayleigh fading environment is given as

$$\ell_1(y) = \sum_{k=0}^{\infty} \Pr\{N=k\} \times \mathbb{E}\left[\prod_{x\in\ell^*} \frac{1}{1+sP_V(y^2+x^2)^{-\alpha_V/2}}\right] \tag{13}$$

The vehicular nodes are distributed using independent and homogeneous PPP. Thus, mean number of points (vehicular nodes) lying on a line segment $2\sqrt{R^2-y^2}$ is given as $2\mu_V\sqrt{R^2-y^2}$ and PDF of the vehicular nodes in the considered length of line segment is given as $f(x) = 1/2\mu_V\sqrt{R^2-y^2}$. The probability that there are k vehicular nodes lying on a line segment $2\sqrt{R^2-y^2}$ is given as $e^{-2\mu_V\sqrt{R^2-y^2}}(2\mu_V\sqrt{R^2-y^2})^k/k!$. Thus, (13) can be expressed as

$$\ell_1(y) = e^{-2\mu_V\sqrt{R^2-y^2}}(2\mu_V\sqrt{R^2-y^2})^k/k! \times \left(\underbrace{\int_{x=-\sqrt{R^2-y^2}}^{\sqrt{R^2-y^2}} \frac{f(x)}{1+sP_V(y^2+x^2)^{-\alpha_e/2}}dx}_{\Psi^*}\right)^k, \tag{14}$$

where x is uniformly distributed between $-\sqrt{R^2-y^2}$ and $\sqrt{R^2-y^2}$ in Ψ^*. Substituting $f(x)$ and after simple mathematical manipulations, we get

$$\ell_1(y) = e^{-2\mu_V\sqrt{R^2-y^2}} \times \frac{\left(2\mu_V\int_{x=0}^{\sqrt{R^2-y^2}} \frac{dx}{1+sP_V(y^2+x^2)^{-\alpha_e/2}}\right)^k}{k!}, \tag{15}$$

Using even function property for Taylor series (i.e., $\sum_{k=0}^{\infty} e^{\mathcal{X}} = \mathcal{X}^k/k!$, we get $\ell_1(y)$ as

$$\ell_1(y) = e^{-2\mu_V\sqrt{R^2-y^2}} \times \exp\left\{2\mu_V\int_{x=0}^{\sqrt{R^2-y^2}} \frac{dx}{1+sP_V(y^2+x^2)^{-\alpha_e/2}}\right\}, \tag{16}$$

The final expression for the Laplace transform of interference from single road excluding a typical road and from roads located at $y \geqslant r_V$ is obtained by simple mathematical manipulations and is expressed as

$$\ell_1(y) = \exp \times \left\{-2\mu_V\int_0^{\sqrt{R^2-y^2}} 1 - \frac{1}{1+sP_V(y^2+x^2)^{-\alpha_e/2}}dx\right\}. \tag{17}$$

Similarly, follow the same procedure to obtained the final expression for the Laplace transform of interference from single road excluding a typical road and from roads located at $y < r_V$ and is expressed as

$$\ell_2(y) = \exp \times \left\{-2\mu_V\int_{\sqrt{r_V^2-y^2}}^{\sqrt{R^2-y^2}} 1 - \frac{1}{1+sP_V(y^2+x^2)^{-\alpha_e/2}}dx\right\}. \tag{18}$$

Note that for $y < r_V$, vehicular nodes will be located on line segments with lengths $[-\sqrt{R^2-y^2}, -\sqrt{r_V^2-y^2}]$ and $[\sqrt{r_V^2-y^2}, \sqrt{R^2-y^2}]$.

The total interference of all the vehicular nodes and roads located in a disc $\mathcal{B}(o,R)$ (excluding a typical road) is computed by integrating $\ell_1(y)$ and $\ell_2(y)$ over the entire given region. Consider the number of roads t_1 intersecting $\mathcal{B}(o,r)$ is a Poisson process with mean $2\pi\lambda_L r$ and the interfering vehicular nodes located at these roads are located in $[r,R]$. Similarly, consider the number of roads t_2 located between disc $\mathcal{B}(o,R)$ and disc $\mathcal{B}(o,r)$ intersecting disc $\mathcal{B}(o,r)$ is also a Poisson process with mean $2\pi\lambda_L(R-r)$ and the interfering vehicular nodes are located in $(0,r]$. Then, the Laplace transform of interference originating from vehicular nodes located on all the roads (excluding typical road) can be expressed as

$$\begin{aligned}
L_{I_{V_L}}(r) &= \sum_{t_1\geqslant 0}^{\infty} e^{-2\pi\lambda_L r}\frac{(2\pi\lambda_L r)^{t_1}}{t_1!}\int_{-r}^{r}\left(\frac{\ell_1(r)}{2r}\right)^{t_1}dr \\
&\quad\times\sum_{t_2\geqslant 0}^{\infty} e^{-2\pi\lambda_L(R-r)}\frac{(2\pi\lambda_L(R-r))^{t_2}}{t_2!} \\
&\quad\times\int_{r}^{R}\left(\frac{2\ell_2(r)}{2(R-r)}\right)^{t_2}dr \\
&\overset{a}{=}\sum_{t_1\geqslant 0}^{\infty} e^{-2\pi\lambda_L r}\int_0^r\frac{(2\pi\lambda_L\ell_1(r))^{t_1}}{t_1!}dr \\
&\quad\times\sum_{t_2\geqslant 0}^{\infty} e^{-2\pi\lambda_L(R-r)}\int_r^R\frac{(2\pi\lambda_L\ell_2(r))^{t_2}}{t_2!}dr \\
&\overset{b}{=}\exp\left\{-2\pi\lambda_L\left(\int_0^r 1-\ell_1(r)dr\right.\right. \\
&\quad\left.\left.+\int_r^R 1-\ell_2(r)dr\right)\right\}. \qquad (19)
\end{aligned}$$

(a) is obtained by simplifying mathematical expression and considering $\int_0^r dr = 2\,r$. (b) is obtained by considering even function property for Taylor series expansion and by further simple mathematical manipulations.

2) INTERFERENCE OF VEHICULAR NODES LOCATED ON A TYPICAL ROAD

The interference of vehicular nodes located at a typical road with $y=0$ can be derived by following the same procedure of $\ell_2(r)$ and is expressed by Laplace transform of interference as

$$L_{I_{V_o}}(r) = \exp\left\{-2\mu_V\int_{r_{V_o}}^{R} 1-\frac{1}{1+sP_V x^{-\alpha_e}}dx\right\}, \qquad (20)$$

where r_{V_o} is the horizontal distance of the serving typical transmitter to the typical receiver.

3) INTERFERENCE OF MBS

The interference of cellular BSs at a typical receiver is a well-known expression given in [34], [35] and is expressed by Laplace transform of interference as

$$\begin{aligned}
L_{I_M}(r) &= \mathbb{E}[e^{-sI_M}] = \mathbb{E}_{h_M,\Phi_M}\left[e^{-\Sigma_{X\in\Phi_M} sP_M h_M X^{-\alpha_M}}\right] \\
&\overset{a}{=}\mathbb{E}_{\Phi_M}\left[\prod_{X\in\Phi_M}\mathbb{E}_{h_M}\left[e^{-sP_M h_M X^{-\alpha_M}}\right]\right] \\
&\overset{b}{=}\exp\left\{-\pi\lambda_M\int_{r>0}^{\infty} 1-\mathbb{E}_{h_M}\left[sh_M P_M X^{-\alpha_M}\right]\right\} \\
&\overset{c}{=}\exp\left\{-2\pi\lambda_M\int_r^R 1-\frac{1}{1+sP_V x^{-\alpha_e}}xdx\right\}, \qquad (21)
\end{aligned}$$

where (a) follows by the definition of the Laplace transform and by considering independence of h_M, (b) follows by considering the property of probability generating functional (PGF) of $f(x)=\mathbb{E}_{h_M}\left[e^{-sP_M h_M X^{-\alpha_M}}\right]$, and (c) follows by transforming the function into polar coordinates.

4) INTERFERENCE OF JAMMERS

Here, interference of clustered-jammers at a receiving entity is derived in terms of Laplace transform of jamming interference L_{I_J}. The jamming interference from various clusters located in the vicinity of a typical entity can be derived as [36]

$$\begin{aligned}
L_{I_J} &= \Psi_a\times\Psi_b \\
&= \overbrace{\exp\{-\lambda_j\int_{\mathcal{R}^2}(1-\exp\{-\bar{c}\beta(z,y)\})dy\}}^{\Psi_a} \\
&\quad\times\overbrace{\int_{\mathcal{R}^2}\exp\{-\bar{c}\beta(z,y)\}f(y)dy}^{\Psi_b}, \qquad (22)
\end{aligned}$$

where $\beta(z,y)=\int_{\mathcal{R}^2}\frac{g(x-y-z)}{g(x-y-z)+g(z)/\tau}f(x)dx$ and Ψ_a is the PGF of clustered-jammers. The PGF is simplified in [14], [15] for clustered-jammers as

$$\begin{aligned}
\Psi_a &= \exp\left\{-\lambda_j\int_{\mathcal{R}^2}(1-\right. \\
&\quad\left.\times\exp\left\{-\bar{c}\int_{\mathcal{R}^2}\frac{g(x-y-z)}{g(x-y-z)+g(z)/\tau}f(x)dx\right\}\right)dy\Bigg\} \\
&\overset{a}{=}\exp\left\{-\lambda_j\int_{\mathcal{R}^2}\left(1-\exp\left\{\int_{\mathcal{R}^2}-\frac{\bar{c}g(y)f(x)dx}{g(y)+g(z)/\tau}\right\}\right)dy\right\} \\
&\overset{b}{=}\exp\left\{-2\pi\lambda_j\int_0^R\left(1-\exp\left\{\frac{-\bar{c}y^{-\alpha_e}}{y^{-\alpha_e}+r^{-\alpha_e}/\tau}\right\}\right)ydy\right\} \\
&\overset{c}{=}\exp\left\{-\lambda_j\pi\tau^{2/\alpha_e}r^2\int_0^R\left(1-\exp\left\{\frac{-\bar{c}}{1+\omega^{\alpha_e/2}}\right\}\right)d\omega\right\},
\end{aligned}$$

where (a) follows by changing variables, (b) follows by mathematical simplification, and (c) follows by considering $\omega = \tau^{-2/\alpha_e}r^{-2}y^2$. Furthermore, Ψ_b is simplified using [37] and is given as $\Psi_b=\int_{\mathcal{R}^2}\exp\{-\bar{c}\beta(z,y)\}f(y)dy = \exp\{-\mathcal{J}r^2\tau^{2/\alpha_e}\frac{2\pi^2}{\alpha_e}\csc(2\pi/\alpha_e)\}$, where $\mathcal{J}=\lambda_j\bar{c}(\pi R_j^2)^{-1}$. The final expression for the Laplace transform of clustered

jamming interference is obtained by substituting the values of Ψ_a and Ψ_b in (22) and is expressed as

$$L_{I_J}(r) = \exp\left\{-\frac{2\pi\lambda_j\bar{c}}{\alpha_e R_j^2}\tau^{2/\alpha_e}\csc\left(\frac{2\pi}{\alpha_e}\right)r^2 - \lambda_j\pi\tau^{2/\alpha_e}r^2 \times \int_0^R\left(1-\exp\left(\frac{-\bar{c}}{1+\omega^{\alpha_e/2}}\right)\right)d\omega\right\}. \quad (23)$$

IV. SUCCESS PROBABILITY ANALYSIS

The probability that SIR of a typical vehicular node without selecting any transmission mode when exceeds a pre-set threshold value is defined as the success probability of V2V communication and is given as

$$P^S(\tau) = \Pr\{\text{SIR}(r) > \tau\}. \quad (25)$$

whereas, the probability that SIR of a typical receiving entity with a specific transmission mode $\mathcal{T}$ exceeds a pre-set threshold value is defined as the success probability under specific selected transmission mode and is given as

$$P^S_{\mathcal{T}}(\tau) = \Pr\{\text{SIR}_{\mathcal{T}}(r) > \tau\}. \quad (26)$$

The success probability directly relates to the reliability of the link connection between entities (e.g., vehicles and MBSs). Thus, the success probability of a typical vehicle with direct transmission is given as the the probability that the SIR of that vehicle exceeds a pre-set threshold value and is expressed as

$$P^S_{\mathcal{D}}(\tau, r_V) = \Pr\{\text{SIR}_{\mathcal{D}}(r_V) > \tau\}. \quad (27)$$

The analytical expression for the success probability of direct transmission in V2V and in the presence of clustered-jammers can be derived using CCDF of SIR and is given as

$$P^S_{\mathcal{D}}(\tau, r_V) = \int_0^R L_{I_{V_L}}(r_V)L_{I_{V_{L_o}}}(r_V)L_{I_J}(r_V)f_{R_V}(r_V)dr_V. \quad (28)$$

The final expression for the success probability of direct transmission is obtained in (24), as shown at the bottom of the page, by substituting the values of $L_{I_{V_L}}(r_V)$, $L_{I_{V_{L_o}}}(r_V)$, $L_{I_J}(r_V)$, and $f_{R_V}(r_V)$, from (19), (20), (23), and (5), respectively in (28) by considering $e = V$ and $r = r_V$.

For cellular-assisted vehicular transmission, the success probability of a typical vehicular node in V2I is given as the the probability that the SIR at an MBS exceeds a pre-set threshold value and is expressed as

$$P^S_{\mathcal{C}}(\tau, r_{V2M}) = \Pr\{\text{SIR}_{\mathcal{C}}(r_{V2M}) > \tau\}. \quad (29)$$

The analytical expression for the success probability of cellular-assisted vehicular transmission in the presence of clustered-jammers at an MBS can be derived as

$$P^S_{\mathcal{C}}(\tau, r_{V2M}) = \int_0^R L_{I_{V_L}}(r_{V2M})L_{I_{V_{L_o}}}(r_{V2M})L_{I_J}(r_{V2M}) \times f_{R_{V2M}}(r_{V2M})dr_{V2M}. \quad (30)$$

Substituting the values of $L_{I_{V_L}}(r)$, $L_{I_{V_{L_o}}}(r)$, $L_{I_J}(r)$, and $f_{R_V}(r)$, from (19), (20), (23), and (5), respectively in (30) by considering $e = V$, $R_M = R_{V2M}$, and $r = r_M = r_{V2M}$, the final expression for the success probability of cellular-assisted vehicular transmission is obtained in (34), as shown at the bottom of the next page.

Similarly, the success probability of a typical test vehicular node with cellular-assisted vehicular transmission in I2V is given as the the probability that the SIR at a typical vehicular node exceeds a pre-set threshold value and is expressed as

$$P^S_{\mathcal{C}}(\tau, r_{M2V}) = \Pr\{\text{SIR}_{\mathcal{C}}(r_{M2V}) > \tau\}. \quad (31)$$

The analytical expression for the success probability of cellular-assisted vehicular transmission in the presence of clustered-jammers at a typical vehicular node can be derived as

$$P^S_{\mathcal{C}}(\tau, r_{M2V}) = \int_0^R L_{I_M}(r_{M2V})L_{I_J}(r_{M2V})f_{R_{M2V}}(r_{M2V})dr_{M2V}. \quad (32)$$

Substituting the values of $L_{I_M}(r)$, $L_{I_J}(r)$, and $f_{R_V}(r)$, from (21), (23), and (5), respectively in (32) by considering $e = M$, $R_M = R_{M2V}$, and $r = r_M = r_{M2V}$, the final expression for the success probability of cellular-assisted vehicular transmission is obtained in (35), as shown at the bottom of the next page.

The overall success probability of cellular-assisted vehicular transmissions is expressed as

$$P^S_{\mathcal{T}}(\tau) = P^S_{\mathcal{D}}(\tau, r_V)\mathcal{A}_D + P^S_{\mathcal{C}}(\tau, r_{V2M})P^S_{\mathcal{C}}(\tau, r_{M2V})\mathcal{A}_C, \quad (33)$$

Substituting the values of $P^S_{\mathcal{D}}(\tau, r_V)$, $\mathcal{A}_D$, $P^S_{\mathcal{C}}(\tau, r_{V2M})$, $P^S_{\mathcal{C}}(\tau, r_{M2V})$, and $\mathcal{A}_C$ from (28), (10), (30), (32), and (12), respectively in (33), we obtain the final expression for the success probability of cellular-assisted vehicular transmission.

V. RESULTS AND DISCUSSION

In this section, we present overall success probability results of cellular-assisted vehicular communications. The analytical results are validated using simulations with 100,000 Monte

$$P^S_{\mathcal{D}}(\tau, r_V) = \int_0^R \exp\left\{-2\pi\lambda_L\left(\int_0^r 1-\ell_1(r)dr + \int_r^R 1-\ell_2(r)dr\right)\right\}\exp\left\{-2\mu_V\int_{r_{V_o}}^R 1 - \frac{1}{1+sP_V x^{-\alpha_V}}dx\right\} \times \exp\left\{-\frac{2\pi\lambda_j\bar{c}}{\alpha_V R_j^2}\tau^{2/\alpha_V}\csc\left(\frac{2\pi}{\alpha_V}\right)r^2 - \lambda_j\pi\tau^{2/\alpha_V}r^2\int_0^R\left(1-\exp\left(\frac{-\bar{c}}{1+\omega^{\alpha_V/2}}\right)\right)d\omega\right\}f_{R_V}(r_V)dr_V \quad (24)$$

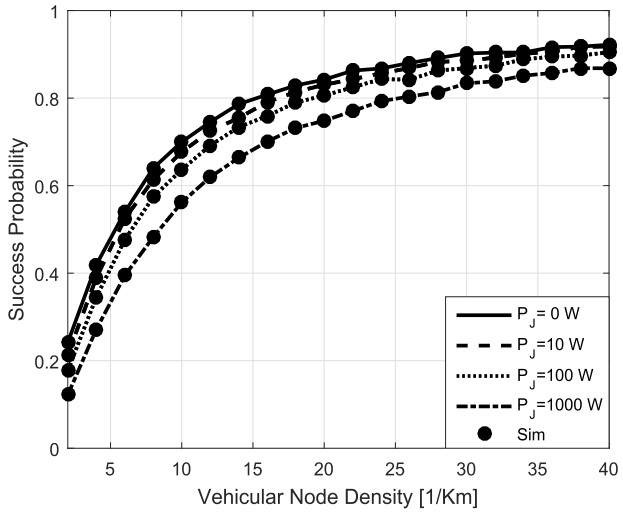

FIGURE 4. Success probability as a function of density of vehicular nodes in the presence of jamming interference.

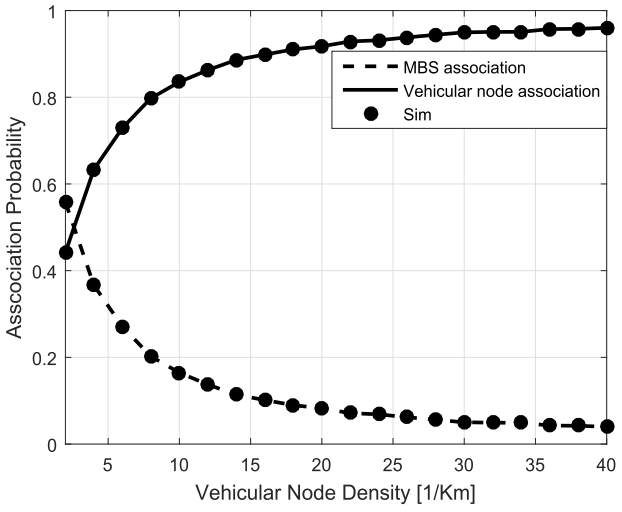

FIGURE 5. Association probability of the transmitting (test) vehicular node as a function of density of vehicular nodes in the presence of jamming interference.

Carlo runs using MATLAB platform. Unless stated otherwise, we consider pathloss exponent $\alpha_M = \alpha_V = 4$. The transmit power of the MBSs, vehicular nodes, and jammers is set to $P_M = 43$ [dBm], $P_V = 23$ [dBm], and $P_J = 10$ [dBm], respectively. The intensity of roads is set to $\lambda_L = 5$ [Km/Km^2] while, the intensity of MBSs, vehicular nodes, and jamming clusters is set to $\lambda_M = 20$ [1/Km^2], $\mu_V = 10$ [1/Km], and $\lambda_j = 10$ [1/Km^2], respectively. The average number of jammers in a cluster is set to $\bar{c} = 4$ and the radius of the clustered-jammers is set to $R_j = 100$ [m]. The system bandwidth is set to $B = 10$ [MHz].

Fig. 4 shows the effect of increasing vehicular node density on the success probability in the presence of jamming nodes. It is shown that the success probability increases by increasing the density of vehicular nodes; however, the success probability of the vehicular networks in the presence of jamming nodes is lower than the success probability of vehicular networks without jamming nodes. Moreover, the success probability further decreases with the increasing power of jamming nodes. Thus, it is suggested to introduce and focus on anti-jamming techniques in cellular-assisted vehicular communications, when the transmission power of the jamming nodes is increased in the network. Note that the success probability increases by increasing the density of vehicular nodes because the distance-dependent pathloss between transmitting test vehicular node and receiving vehicular node decreases which increases the received SIR and the success probability.

Fig. 5 shows the effect of increasing vehicular node density on the association probability of transmitting vehicular node with the cellular BS and typical receiving vehicular node. It is shown that the association probability of the direct transmission (i.e., vehicular node association) increases by

$$P_C^S(\tau, r_{V2M}) = \int_0^R \exp\left\{-2\pi\lambda_L\left(\int_0^r 1-\ell_1(r)dr + \int_r^R 1-\ell_2(r)dr\right)\right\} \times \exp\left\{-2\mu_V\int_{r_{V_o}}^R 1-\frac{1}{1+sP_V x^{-\alpha_M}}dx\right\} \times \exp\left\{-\frac{2\pi\lambda_j\bar{c}}{\alpha_M R_j^2}\tau^{2/\alpha_M}\csc\left(\frac{2\pi}{\alpha_M}\right)r^2 - \lambda_j\pi\tau^{2/\alpha_M}r^2\int_0^R\left(1-\exp\left(\frac{-\bar{c}}{1+\omega^{\alpha_M/2}}\right)\right)d\omega\right\} \times f_{R_{V2M}}(r_{V2M})dr_{V2M} \tag{34}$$

$$P_C^S(\tau, r_{M2V}) = \int_0^R \exp\left\{-2\pi\lambda_M\int_r^R 1-\frac{1}{1+sP_V x^{-\alpha_V}}xdx\right\}\exp\left\{-\frac{2\pi\lambda_j\bar{c}}{\alpha_V R_j^2}\tau^{2/\alpha_V}\csc\left(\frac{2\pi}{\alpha_V}\right)r^2 - \lambda_j\pi\tau^{2/\alpha_V}r^2 \times \int_0^R\left(1-\exp\left(\frac{-\bar{c}}{1+\omega^{\alpha_V/2}}\right)\right)d\omega\right\}f_{R_{M2V}}(r_{M2V})dr_{M2V} \tag{35}$$

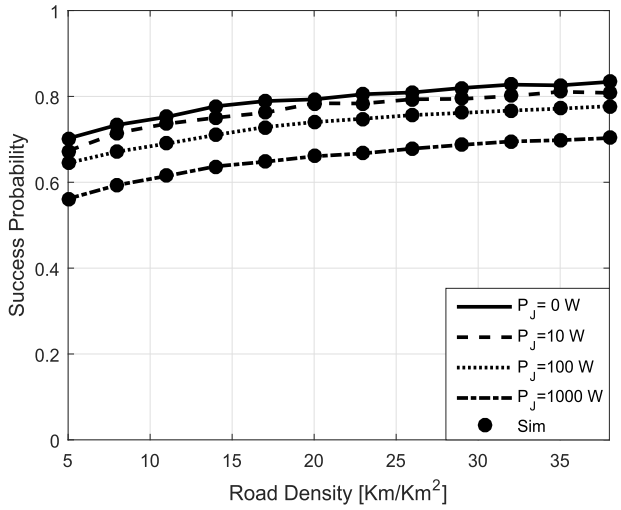

FIGURE 6. Success probability as a function of density of roads in the presence of jamming interference.

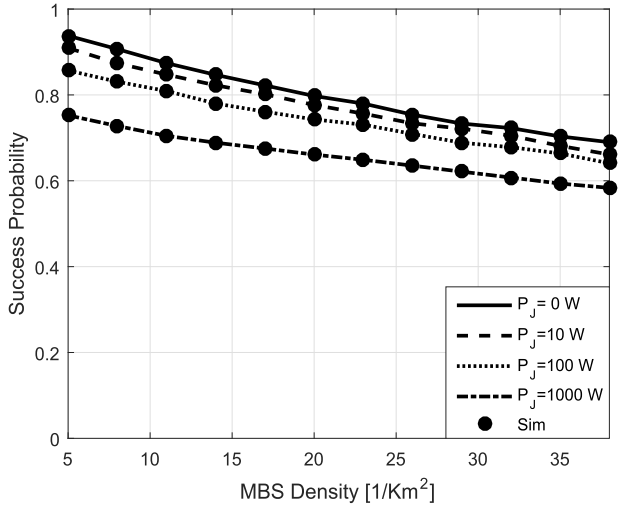

FIGURE 7. Success probability as a function of density of cellular BSs in the presence of jamming interference.

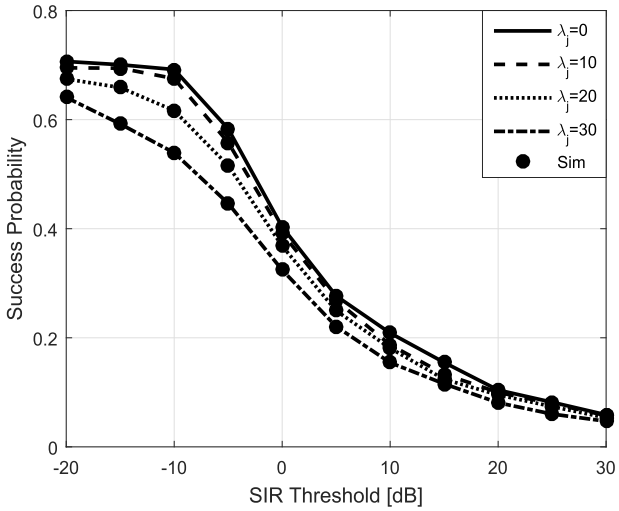

FIGURE 8. Success probability as a function of SIR threshold value in the presence of jamming interference.

increasing the density of vehicular nodes in comparison with the association probability of the cellular-assisted vehicular transmission (i.e., MBS association). This is because the distance between the transmitting and receiving vehicular node decreases by increasing the density of vehicular nodes which increases the received power at the typical vehicular node in comparison with the received power at the MBS. Moreover, it is also shown that at a lower density of vehicular nodes both MBS and vehicular node association are used by vehicular networks.

Fig. 6 shows the effect of increasing road density on the success probability in the presence of jamming nodes. It is shown that the success probability increases by increasing the density of roads. However, the success probability of the vehicular networks in the presence of jammers is lower than the success probability of vehicular networks without jammers. Moreover, the success probability is further decreased by increasing the power of jamming nodes. The success probability of vehicular networks increases with road density because the distance-dependent pathloss between transmitting and receiving entities decreases by increasing the density of roads in the considered region which increases the SIR and the probability of success in coverage.

Fig. 7 shows the effect of increasing the density of MBSs on the success probability in the presence of jammers. It is shown that the success probability decreases by increasing the MBS density. This is because, with the increase in the density of cellular BSs, interference power also increases which decreases the SIR and success probabilities. Moreover, the success probability is further decreased by increasing the power of jamming nodes.

Fig. 8 shows the effect of the SIR threshold value on the success probability in the presence of jamming clusters. It is shown that the success probability decreases by increasing the SIR threshold value. It is also shown that the success probability further decreases by increasing the density of jamming clusters because with the increasing number of jamming clusters in the region of interest, the cumulative jamming power will increase which will increase the network interference and as a result, success probability will decrease. Thus, it is suggested to introduce and focus on anti-jamming techniques in cellular-assisted vehicular communications, when the number of jamming clusters is increased in the network.

VI. CONCLUSION

In this paper, jamming interference is analyzed for cellular-assisted vehicular communications. MBSs are modeled using independent and 2D homogeneous PPP while, vehicles, RSUs, and pedestrians are modeled using 1D homogeneous PLP. The jammers are placed in clusters using MCP and the impact of jamming interference on vehicular networks is obtained in terms of the success probability. It is

shown that jammers severely disrupt the success probability of vehicular networks. It is also shown that the network's performance decreases by increasing the density of jamming clusters and their transmission power. Therefore, the main focus of the network operators should be to introduce anti-jamming, when the transmission power of the jammers and the number of jamming clusters in the network increase.

APPENDIX A
DERIVATION OF (5)

The distance between typical vehicular transmitter and vehicular receiver considers that there is no vehicular node in a disc of radius r_V centered at origin (i.e., $\mathcal{B}(o, r_V)$) that can create interference. The test vehicle can be located either on the same typical line (road) where typical receiving vehicle is present or it can be present on any other line (road). The shortest distance of the vehicular transmitting (test) and receiving (typical) node is given as cumulative distance distribution (CDF) $F_{R_V}(r_V)$ in [31] and is expressed as

$$\begin{aligned} F_{R_V}(r_V) &= \Pr\{R_V \leqslant r_V\} \\ &= 1 - \Pr\{R_V > r_V\} \\ &= 1 - \overbrace{\Pr\{\mathcal{N}_L(\mathcal{B}(o, r_V)) = 0\}}^{\Psi_1} \overbrace{\Pr\{N_{L_o}(-r_V, r_V)\}}^{\Psi_2}, \end{aligned} \tag{36}$$

where $\Pr\{\mathcal{N}_L(\mathcal{B}(o, r_V)) = 0\}$ represents that the number of vehicular nodes on lines (roads) in a point process Φ_L centered at origin with radius r_V is zero and $\Pr\{N_{L_o}(-r_V, r_V)\}$ represents that the number of vehicular nodes located on a typical line L_o with distance $[-r_V, r_V]$. $\Pr\{\mathcal{N}_L(\mathcal{B}(o, r_V)) = 0\}$ can be derived by finding the probability that there are k lines (roads) present in a disc $\mathcal{B}(o, r_V)$ and is given as $\Pr\{\mathcal{N}_{roads}(\mathcal{B}(o, r_V)) = k\}$. Then, for each of the k-th line, find the probability that the number of vehicular nodes on that road is zero (i.e., $\Pr\{N_V(road_i) = 0\}$). $\Pr\{\mathcal{N}_L(\mathcal{B}(o, r_V)) = 0\}$ is derived as

$$\begin{aligned} \Psi_1 &= \sum_{k=0}^{\infty} \Pr\{\mathcal{N}_{roads}(\mathcal{B}(o, r_V)) = k\} \\ &\quad \times \prod_{i=1}^{k} \Pr\{N_V(road_i) = 0\} \\ &\overset{a}{=} \sum_{k=0}^{\infty} \frac{\exp\left(-2\pi\lambda_L r_V\right)\left(2\pi\lambda_L r_V\right)^k}{k!} \\ &\quad \times \left(\int_{y=-r_V}^{r_V} \frac{e^{-2\mu_V\sqrt{r_V^2-y^2}}}{2r_V} dy \right)^k \\ &\overset{b}{=} \exp\left(-2\pi\lambda_L r_V\right) \sum_{k=0}^{\infty} \frac{\left(\pi\lambda_L \int_{-r_V}^{r_V} e^{-2\mu_V\sqrt{r_V^2-y^2}} dy\right)^k}{k!} \\ &\overset{c}{=} \exp\left(-2\pi\lambda_L r_V\right) \exp\left(\pi\lambda_L \int_{-r_V}^{r_V} e^{-2\mu_V\sqrt{r_V^2-y^2}} dy\right) \\ &\overset{d}{=} \exp\left(-2\pi\lambda_L \int_0^{r_V} \left(1 - e^{-2\mu_V\sqrt{r_V^2-y^2}}\right) dy\right), \end{aligned} \tag{37}$$

where (a) represents that the number of roads intersecting a disc of radius r_V centered at the origin is Poisson distributed with average roads given as $2\pi\lambda_L r_V$ and the number of vehicular nodes that are uniformly distributed between $[-r_V, r_V]$ and located on a road is also Poisson distributed with average vehicular nodes per road given as $2\mu_V\sqrt{r_V^2 - y^2}$. (b) is obtained by simple mathematical manipulations, (c) is obtained using even function property for Taylor series (i.e., $\sum_{k=0}^{\infty} e^{\mathcal{X}} = \mathcal{X}^k/k!$), and (d) is obtained by simple mathematics and considering $\int_{-r_V}^{r_V} = 2r_V$. Thus, the CDF of distance between a typical receiving and transmitting vehicular node is obtained by substituting $\Psi_2 = \exp(-2\mu_V r_V)$ and (37) in (36) and is expressed as

$$\begin{aligned} F_{R_V}(r_V) = 1 - \exp&\left(-2\pi\lambda_L \int_0^{r_V} 1 - e^{-2\mu_V\sqrt{r_V^2-y^2}} dy\right) \\ &\times \exp(-2\mu_V r_V). \end{aligned} \tag{38}$$

REFERENCES

[1] S. Gyawali, S. Xu, Y. Qian, and R. Q. Hu, "Challenges and solutions for cellular based V2X communications," *IEEE Commun. Surveys Tuts.*, vol. 23, no. 1, pp. 222–255, Oct. 2021.

[2] C. R. Storck and F. Duarte-Figueiredo, "A survey of 5G technology evolution, standards, and infrastructure associated with vehicle-to-everything communications by Internet of Vehicles," *IEEE Access*, vol. 8, pp. 117593–117614, 2020.

[3] *Study on LTE-Based V2X Services (Release 14)*, document TR36.885, 3GPP, Jul. 2016. [Online]. Available: https://portal.3gpp.org/desktopmodules/Specifications/SpecificationDetails.aspx?specificationId=2934

[4] M. N. Sial, Y. Deng, J. Ahmed, A. Nallanathan, and M. Dohler, "Stochastic geometry modeling of cellular V2X communication over shared channels," *IEEE Trans. Veh. Technol.*, vol. 68, no. 12, pp. 11873–11887, Dec. 2019.

[5] T. Kimura, "Performance analysis of cellular-relay vehicle-to-vehicle communications," *IEEE Trans. Veh. Technol.*, vol. 70, no. 4, pp. 3396–3411, Apr. 2021.

[6] M. Hasan, S. Mohan, T. Shimizu, and H. Lu, "Securing vehicle-to-everything (V2X) communication platforms," *IEEE Trans. Intell. Vehicles*, vol. 5, no. 4, pp. 693–713, Dec. 2020.

[7] S. Li, J. Zhao, W. Tan, and C. You, "Optimal secure transmit design for wireless information and power transfer in V2X vehicular communication systems," *AEU Int. J. Electron. Commun.*, vol. 118, May 2020, Art. no. 153148.

[8] H. Zhou, W. Xu, J. Chen, and W. Wang, "Evolutionary V2X technologies toward the internet of vehicles: Challenges and opportunities," *Proc. IEEE*, vol. 108, no. 2, pp. 308–323, Feb. 2020.

[9] M. H. C. Garcia, A. Molina-Galan, M. Boban, J. Gozalvez, B. Coll-Perales, T. Sahin, and A. Kousaridas, "A tutorial on 5G NR V2X communications," *IEEE Commun. Surveys Tuts.*, vol. 23, no. 3, pp. 1972–2026, 2021.

[10] M. Gonzalez-Martín, M. Sepulcre, R. Molina-Masegosa, and J. Gozalvez, "Analytical models of the performance of C-V2X mode 4 vehicular communications," *IEEE Trans. Veh. Technol.*, vol. 68, no. 2, pp. 1155–1166, Feb. 2019.

[11] H. Hasrouny, A. E. Samhat, C. Bassil, and A. Laouiti, "VANet security challenges and solutions: A survey," *Veh. Commun.*, vol. 7, pp. 7–20, Jan. 2017.

[12] V. H. LA and A. Cavalli, "Security attacks and solutions in vehicular ad hoc networks: A survey," *Int. J. Ad Hoc Netw. Syst.*, vol. 4, no. 2, pp. 1–20, Apr. 2014.

[13] N. K. Chaubey, "Security analysis of vehicular ad hoc networks (VANETs): A comprehensive study," *Int. J. Secur. Appl.*, vol. 10, no. 5, pp. 261–274, May 2016.

[14] M. Arif, S. Wyne, K. Navaie, M. S. Haroon, and S. Qureshi, "Clustered jamming in aerial HetNets with decoupled access," *IEEE Access*, vol. 8, pp. 142218–142228, 2020.

[15] M. Arif, S. Wyne, K. Navaie, M. S. Haroon, and S. Qureshi, "Dual connectivity in decoupled aerial HetNets with reverse frequency allocation and clustered jamming," *IEEE Access*, vol. 8, pp. 221454–221467, 2020.
[16] M. S. Sheikh, J. Liang, and W. Wang, "A survey of security services, attacks, and applications for vehicular ad hoc networks (VANETs)," *Sensors*, vol. 19, no. 16, p. 3589, 2019.
[17] Y. P. Fallah, C.-L. Huang, R. Sengupta, and H. Krishnan, "Analysis of information dissemination in vehicular ad-hoc networks with application to cooperative vehicle safety systems," *IEEE Trans. Veh. Technol.*, vol. 60, no. 1, pp. 233–247, Oct. 2010.
[18] Y. Yao, L. Rao, and X. Liu, "Performance and reliability analysis of IEEE 802.11p safety communication in a highway environment," *IEEE Trans. Veh. Technol.*, vol. 62, no. 9, pp. 4198–4212, Nov. 2013.
[19] C. Han, M. Dianati, R. Tafazolli, R. Kernchen, and X. Shen, "Analytical study of the IEEE 802.11p MAC sublayer in vehicular networks," *IEEE Trans. Intell. Transp. Syst.*, vol. 13, no. 2, pp. 873–886, Jun. 2012.
[20] Z. Tong, H. Lu, M. Haenggi, and C. Poellabauer, "A stochastic geometry approach to the modeling of DSRC for vehicular safety communication," *IEEE Trans. Intell. Transp. Syst.*, vol. 17, no. 5, pp. 1448–1458, May 2016.
[21] T. V. Nguyen, F. Baccelli, K. Zhu, S. Subramanian, and X. Wu, "A performance analysis of CSMA based broadcast protocol in VANETs," in *Proc. IEEE INFOCOM*, Apr. 2013, pp. 2805–2813.
[22] C.-S. Choi and F. Baccelli, "An analytical framework for coverage in cellular networks leveraging vehicles," *IEEE Trans. Commun.*, vol. 66, no. 10, pp. 4950–4964, Oct. 2018.
[23] V. V. Chetlur and H. S. Dhillon, "On the load distribution of vehicular users modeled by a Poisson line cox process," *IEEE Wireless Commun. Lett.*, vol. 9, no. 12, pp. 2121–2125, Dec. 2020.
[24] H. S. Dhillon and V. V. Chetlur, "Poisson line cox process: Foundations and applications to vehicular networks," *Synth. Lectures Learn., Netw., Algorithms*, vol. 1, no. 1, pp. 1–149, Jun. 2020.
[25] S. Feng and S. Haykin, "Anti-jamming V2V communication in an integrated UAV-CAV network with hybrid attackers," in *Proc. IEEE Int. Conf. Commun. (ICC)*, May 2019, pp. 1–6.
[26] S. Feng and S. Haykin, "Cognitive risk control for anti-jamming V2V communications in autonomous vehicle networks," *IEEE Trans. Veh. Technol.*, vol. 68, no. 10, pp. 9920–9934, Oct. 2019.
[27] L. Jia, Y. Xu, Y. Sun, S. Feng, L. Yu, and A. Anpalagan, "A multi-domain anti-jamming defense scheme in heterogeneous wireless networks," *IEEE Access*, vol. 6, pp. 40177–40188, 2018.
[28] D. Kosmanos, A. Argyriou, and L. Maglaras, "Estimating the relative speed of RF jammers in VANETs," *Secur. Commun. Netw.*, vol. 2019, pp. 1–18, Nov. 2019.
[29] S. N. Chiu, D. Stoyan, W. S. Kendall, and J. Mecke, *Stochastic Geometry and its Applications*. Hoboken, NJ, USA: Wiley, 2013.
[30] M. Qasim, M. S. Haroon, M. Imran, F. Muhammad, and S. Kim, "5G cellular networks: Coverage analysis in the presence of inter-cell interference and intentional jammers," *Electronics*, vol. 9, no. 9, p. 1538, Sep. 2020.
[31] S. Guha, "Cellular-assisted vehicular communications: A stochastic geometric approach," M.S. thesis, Dept. Elect. Comput. Eng., Virginia Polytech. Inst. State Univ., Blacksburg, VA, USA, 2016.
[32] J. P. Jeyaraj and M. Haenggi, "Cox models for vehicular networks: SIR performance and equivalence," *IEEE Trans. Wireless Commun.*, vol. 20, no. 1, pp. 171–185, Jan. 2021.
[33] V. V. Chetlur and H. S. Dhillon, "Coverage analysis of a vehicular network modeled as Cox process driven by Poisson line process," *IEEE Trans. Wireless Commun.*, vol. 17, no. 7, pp. 4401–4416, Jul. 2018.
[34] J. G. Andrews, A. K. Gupta, and H. S. Dhillon, "A primer on cellular network analysis using stochastic geometry," 2016, *arXiv:1604.03183*.
[35] M. Haenggi, *Stochastic Geometry for Wireless Networks*. Cambridge, U.K.: Cambridge Univ. Press, 2012.
[36] R. K. Ganti and M. Haenggi, "Interference and outage in clustered wireless ad hoc networks," *IEEE Trans. Inf. Theory*, vol. 55, no. 9, pp. 4067–4086, Sep. 2009.
[37] Y. Wang and Q. Zhu, "Modeling and analysis of small cells based on clustered stochastic geometry," *IEEE Commun. Lett.*, vol. 21, no. 3, pp. 576–579, Mar. 2017.

MOHAMMAD ARIF received the B.S. degree in electrical engineering from the University of Engineering and Technology, Peshawar, Pakistan, in 2012, and the M.S. and Ph.D. degrees in electrical engineering from COMSATS University Islamabad (CUI), Islamabad, Pakistan, in 2014 and 2021, respectively.

His research interests include cellular-assisted vehicular communications, aerial and terrestrial heterogeneous networks, dual connectivity, uplink and downlink interference management, reverse frequency allocation, indoor localization, signal processing, and channel coding.

WOOSEONG KIM received the Ph.D. degree in computer science from the UCLA. He was a Researcher with Samsung Electronics, Hyundai Motor, LG Electronics, and SK Hynix Semiconductor. He is currently a Professor with the Computer Engineering Department, Gachon University, South Korea. He had standardization activity in several SDOs, such as 3GPP, ITU, TTA, and ETSI. His research interests include multi-hop ad hoc networks, LTE and 5G wireless telecommunication systems, wireless LAN, SDN/NFV, and the IoT protocols.

SADIA QURESHI received the M.S. degree in electrical engineering from the University of Engineering and Technology, Peshawar, Pakistan. She is currently pursuing the Ph.D. degree with the School of Electrical and Data Engineering, University of Technology Sydney, Sydney. She is also a full-time Research Scholar with the School of Electrical and Data Engineering, University of Technology Sydney. Her research interests include vehicular communications, heterogeneous networks, signal processing, wireless sensor networks, software-defined networking, and optical networks.